Langmuir

Article

pubs.acs.org/Langmuir

Fabrication of Planar Colloidal Clusters with Template-Assisted Interfacial Assembly

Christopher L. Wirth,*[,†,∥] Michael De Volder,[‡] and Jan Vermant[†,§]

[†]Department of Chemical Engineering, KU Leuven, W. de Croylaan 46, B-3001 Leuven, Belgium

[‡]Department of Engineering, Cambridge University, 17 Charles Babbage Road, CB3 0FS, Cambridge, United Kingdom

[§]Laboratory for Soft Materials, Department of Materials, ETH Zürich, Vladimir Prelog Weg 5, CH-8093 Zurich, Switzerland

Supporting Information

ABSTRACT: The synthesis of nanoparticle clusters, also referred to as colloidal clusters or colloidal molecules, is being studied intensively as a model system for small molecule interactions as well as for the directed self-assembly of advanced materials. This paper describes a technique for the interfacial assembly of planar colloidal clusters using a combination of top-down lithographic surface modification and bottom-up Langmuir–Blodgett deposition. Micrometer sized polystyrene latex particles were deposited onto a chemically modified substrate from a decane–water interface with Langmuir–Blodgett deposition. The surface of the substrate contained hydrophilic domains of various size, spacing, and shape, while the remainder of the substrate was hydrophobic. Particles selectively deposited onto hydrophilic regions from the decane–water interface. The number of deposited particles depended on the size of each patch, thereby demonstrating that tuning cluster size is possible by engineering patch geometry. Following deposition, the clusters were permanently bonded with temperature annealing and then removed from the substrate via sonication. The permanently bonded planar colloidal clusters were stable in an aqueous environment and at a decane–water interface laden with isotropic colloidal particles. The method is a simple and fast way to synthesize colloidal clusters with few limitations on particle chemistry, composition, and shape.

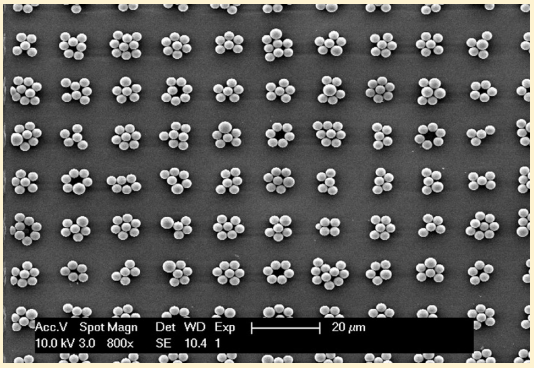

INTRODUCTION

Substantial effort has been invested in developing assembly techniques for the synthesis of colloidal clusters of varying shape.[1−11] A colloidal cluster assembled from individual particles is often referred to as a "colloidal molecule", especially when aggregation is sufficiently controlled such that the cluster structure resembles molecular structure. For example, a dimer of identically sized spherical colloidal particles is analogous to a molecule of H_2.[4,7] Not only do colloidal clusters serve as a model system for studying small molecules whose interactions are dictated by cluster geometry and variations in surface chemistry, but such clusters can also serve as components in the directed self-assembly of advanced materials.[12] Anisotropic colloidal clusters in either 3D (i.e., in the bulk) or 2D (i.e., on a surface) have been fabricated in a number of ways, including tuning depletion interactions in "lock and key" colloids,[13] assembly via spatial templating of the substrate,[2,6] controlled evaporation of one phase in an emulsion,[1,9] and irreversible attraction between particles or between particles and a substrate that have been modified to have a specific colloidal attraction.[14−20] These studies have illustrated the wide structural diversity and utility of geometrically complex colloidal clusters.

The 2D directed self-assembly of colloidal particles on a substrate is a closely related research area that is often used for the fabrication of colloidal clusters. There is a large body of literature in this area focused on the assembly of various colloidal particles, including polystyrene spheres,[15,17] nanorods,[21,22] and carbon nanotubes.[23,24] This work is motivated by a variety of engineering and scientific applications, ranging from the synthesis of 2D crystals with unique optical properties[25] to the hierarchal assembly of nanomaterials.[26] Directed self-assembly is usually guided by a template that is either chemical or physical in nature. A chemical template uses a specific attraction to guide assembly, such as a substrate with regions of surface charge opposite from that of the depositing particles.[15,17,20] Aizenberg et al.[15] showed that well-controlled patterned colloidal deposition could be achieved with substrates that had been micropatterned with self-assembled monolayers to produce cationic and anionic regions. Physical templates have also been used to achieve similar results without requiring the modification of either the particle or substrate to have a specific chemical attraction. For instance, colloidal clusters are produced by trapping particles in wells (i.e., the physical template)[2] during the slow evaporation of a sessile drop containing those particles. The technique is effective and has

Received: November 7, 2014
Revised: January 16, 2015
Published: January 29, 2015

DOI: 10.1021/la504383m
Langmuir 2015, 31, 1632−1640

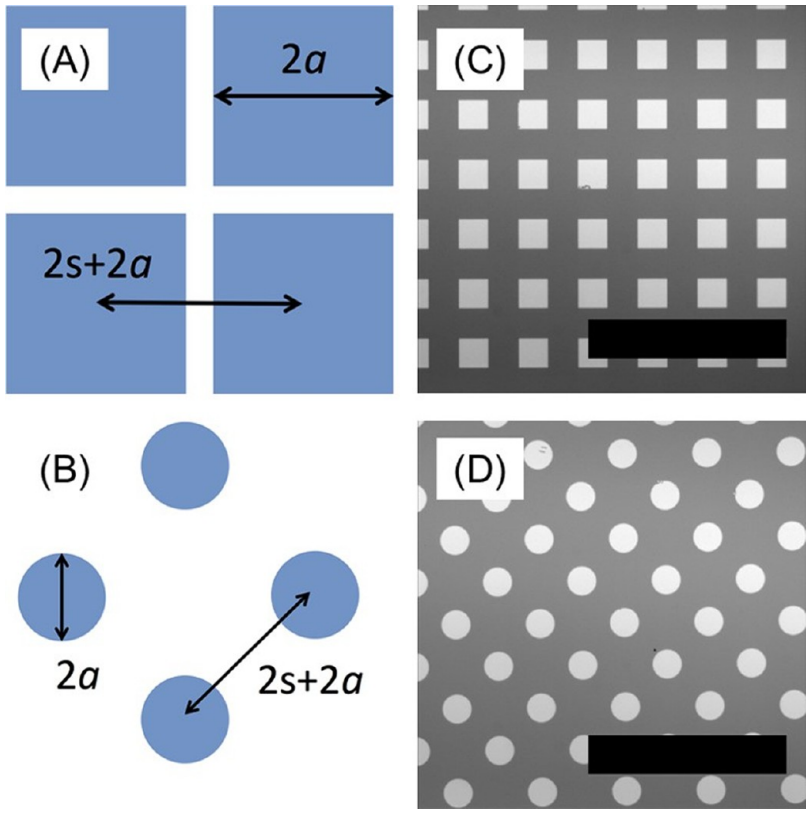

Figure 1. Geometry of patterns. A single wafer was modified to have hydrophilic (A) squares and (B) circles with width or diameter 2*a*, respectively. The nearest neighbor separation distance of hydrophilic patches was 2*s*. (C,D) Optical micrographs of the wafer prior to the deposition of colloidal particles.

the advantage of being generally applicable to a variety of particle compositions because no specific chemical interactions are required. However, the procedure typically requires the slow evaporation of a fluid and is also somewhat limited by the requirement of a precisely machined substrate. An improved technique for the 2D directed self-assembly of colloidal particles would combine the best aspects of existing techniques and provide an effective first step to the fabrication of geometrically complex colloidal clusters.

Here, we present a simple and fast technique that combines substrate modification with interfacial colloidal assembly to synthesize planar colloidal clusters. A Langmuir−Blodgett (LB) deposition technique was used to assemble micrometer-scale polystyrene particles onto a patterned silicon substrate from an oil−water interface. The substrate was patterned with hydrophilic patches, while the remainder of the wafer was hydrophobic. Particles selectively deposited onto hydrophilic regions to form planar colloidal clusters with a size that depended on the patch size. Following deposition, the clusters were permanently bonded via annealing and removed from the substrate. The clusters were stable when redispersed in the bulk and at a decane−water interface. The LB deposition process was fast (linear substrate speed of 1 cm/min) and robust. In addition, the process could be made scalable by using a bottom-up route for the chemical modification of the substrate, rather than a top-down lithographic technique. Further, the chemically modified substrates can be recycled with only mild cleaning between each cycle. There are few limitations on particle chemistry, composition, or shape because no specific chemical interactions were used to induce assembly. The primary requirements are that particles are stable against flocculation while located at a fluid−fluid interface and that the material has a glass transition temperature, which allows for coalescence and permanent bonding of neighboring deposited particles when heated. Although we are not the first to use LB deposition[27−34] or the modification of a substrate to have hydrophobic and hydrophilic domains[35,36] for the assembly of colloidal particles, the technique presented herein is novel in its combination of the two and capitalizes on the advantages of each technique. We present a theoretical framework to analyze our experimental results and demonstrate how the size of clusters can be tuned by engineering the template geometry. This work further illustrates the potential of engineering both fluid−fluid and fluid−solid interfaces for the directed self-assembly of colloidal particles.

THEORY

A. Wetting of a Chemically Patterned Substrate.

Experiments consisted of depositing particles from a decane−water interface onto a chip that had been modified to have hydrophilic and hydrophobic regions of varying geometry. Each geometry was an array of either circular or square hydrophilic patches, with a characteristic length scale a and separation distance $2s$, as shown in Figure 1. Particle deposition occurred as the three-phase contact line moved over hydrophilic patches, as shown schematically in Figure 2. The patches illustrated in Figure 2 are located on a substrate with a reference frame that moves with the patches, such that the three phase contact line moves steadily in the $(-)y$ direction (see Figure 2A). Once in the vicinity of the hydrophilic circles, the contact line pins on the $(+)y$ perimeter edge, but remains mobile in the hydrophobic regions separating the patches (Figure 2B). Thus, there

DOI: 10.1021/la504383m
Langmuir 2015, 31, 1632−1640

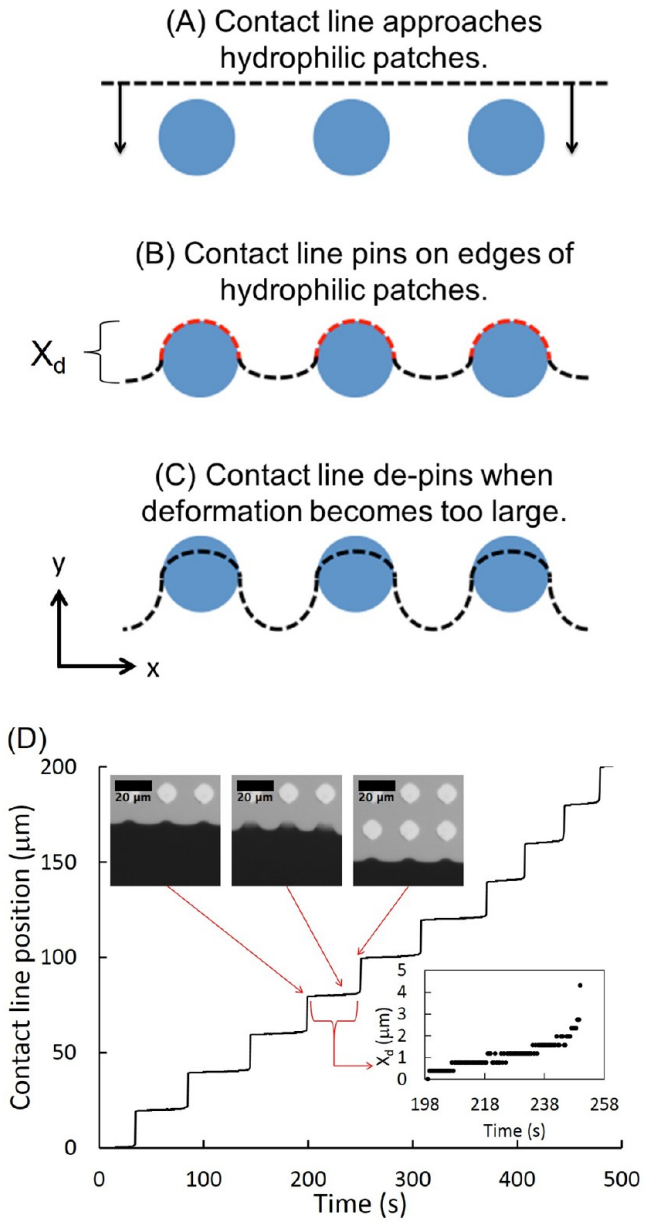

Figure 2. Contact line dynamics. Consider three hydrophilic patches (blue circles) positioned (A) below a receding three phase contact line. (B) The contact line pins on the leading edge of the three hydrophilic patches, but remains mobile in the hydrophobic regions, thereby deforming a distance X_d. (C) The deformation becomes too large and the contact line depins. (D) This process was visualized with an evaporating sessile drop containing gold nanorods. The position of the three phase contact line was tracked during the evaporation process; the pinning/depinning process caused the stair pattern. (D, Inset) The deformation of the contact line plotted as a function of time for one depinning step.

is a deformation X_d between the pinned and mobile portions of the contact line. The deformation grows as the mobile portion of the contact line continues to move downward until there is depinning that relaxes the deformation (Figure 2C). An existing model considers the energetic contributions to the pinning/depinning process to include adhesion and the deformation of the contact line in the region between patches.[37−39] The energy ε_a associated with adhesion of water to the hydrophilic patch for a receding contact line is[37]

$$\varepsilon_a = \gamma A_w(1 + \cos\theta_0) \quad (1)$$

where γ is the interfacial tension of the fluid, A_w is the wetted area of the patch, and θ_0 is the contact angle of the fluid on the patch. The deformation of the contact line was approximated as a linear elastic deformation; the energy associated with this deformation ε_d is[38]

$$\varepsilon_d = \frac{kX_d^2}{2} \quad (2)$$

$$k = \frac{\kappa}{\ln\left(1 + \frac{1}{d}\right)} = \frac{\pi\gamma\theta_c^2}{2\ln\left(1 + \frac{1}{d}\right)} \quad (3)$$

where k is the elastic spring constant, l is the patch separation distance, d is the patch width, γ is the surface tension of the fluid, and θ_c is the contact angle for the homogeneous hydrophilic surface. The appropriate patch separation distance to use in eq 2 depends on the orientation of the chip relative to the fluid−fluid interface during deposition. Here, the separation distance $2s$ was used for square geometries when calculating the reduced spring constant, but the diagonal $2\sqrt{2}s$ was used for circular geometries. Equations 1−3 provide a direct relationship between the geometry of the patterned substrate and the spring constant. Namely, the reduced spring constant, k/κ, depends only on the characteristic length scale and separation distance of the patches comprising the pattern.

EXPERIMENTAL SECTION

A 4 in. silicon wafer was patterned with hydrophilic chromium regions using a standard lift-off process (lift off resist LOR 1A and positive resist IX845 followed by PVD deposition of 30 nm Chromium). Following fabrication, the wafer was cleaned by submerging it in a solution of 150 mL sulfuric acid and 50 mL of hydrogen peroxide (i.e. piranha solution) for 17 min, which balanced the amount of time required to achieve sufficient cleanliness while avoiding etching away the 30 nm chromium layer. Following the cleaning step, the wafer was rinsed with approximately 400 mL of ultrapure water (>18.2 MOhm cm) and then dried under vacuum at 100 °C for 3 h. Next, the wafer was placed in a solution of ∼0.01 g/mL of dichlorodimethylsilane (DCDMS) in cyclohexane for 6 h to make the nonchromium regions hydrophobic. Following the silanization reaction, the wafer was rinsed with acetone, ethanol, and deionized water in that order and dried under vacuum at 100 °C for 1 h. A single wafer contained ∼10 chips, each of which could be used for approximately six experiments with only mild cleaning between each cycle (see Section C of the Supporting Information (SI) for more details on chip recycling).

Particles used in this study were sulfate-modified polystyrene latex particles obtained from Life Technologies (Lot #1459571) with a mean diameter of 2.9 μm and a surface charge density of 9.7 μC/cm^2 according to the certificate of analysis. Prior to deposition, the particles were centrifuged and redispersed in ultrapure water seven times to remove contaminants. Particle washing is key to maintaining a strong dipolar force between particles at interfaces;[40] without washing, a small fraction of particles will often irreversibly aggregate while pinned at the oil−water interface. Next, the particle solution was diluted with 70:30 ultrapure water:isopropyl alcohol (IPA) until the final concentration of the particle solution was ∼10^8 particles/mL. Decane was obtained from ACROS and filtered with two-stages of Al_2O_3 powder to remove polar components prior to use.

LB deposition was conducted with the dipper of a NIMA LB Trough Type 611 from a small cup that was sufficiently deep for the substrate. Initially, 60 mL of ultrapure water was added to the vessel. Next, the chip (a section of the wafer) was moved downward into the water until the three-phase contact line was just above the geometry to which particles would be deposited. Next, between 8 and 10 mL of decane was added; the volume of decane was adjusted such that the

DOI: 10.1021/la504383m
Langmuir 2015, 31, 1632−1640

decane−air interface did not touch the dipping arm. The decane layer thickness was approximately 5 mm (see Figure 3). Finally, the particle

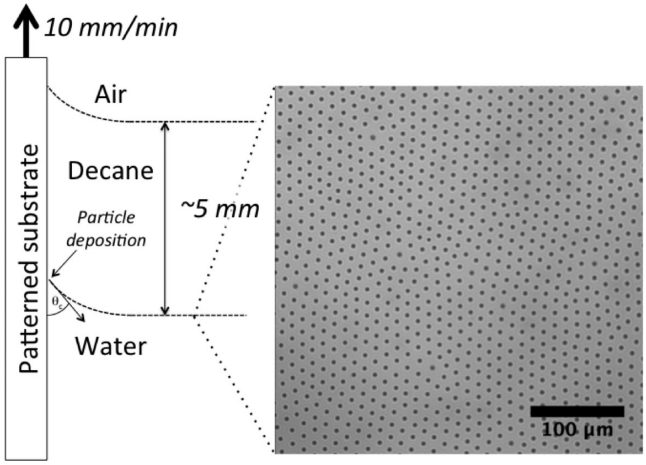

Figure 3. LB deposition from a decane−water interface. Colloidal particles were deposited from the decane−water interface onto a patterned substrate. The three-phase contact angle for the water−decane−substrate and decane−air−substrate were determined by the local pattern of the substrate; here, both angles were drawn <90°. The decane layer was approximately 5 mm thick, although this varied slightly from experiment to experiment depending on the amount of space available for the dipper apparatus. The micrograph shows micrometer sized polystyrene particles pinned to a decane−water interface.

solution was gently added with a 200 μL pipet that was inserted into the decane layer, being careful not to allow the pipet to penetrate the water subphase. Decane−water was used as the fluid−fluid interface to deposit particles from because it is known that there is a substantial enhancement of the electrostatic interactions, with strong and long ranged dipolar repulsion between colloids located at a decane−water interface.[41−43] The strong dipolar repulsion between particles is key to producing a highly ordered and stable monolayer at the interface. A monolayer stable against flocculation will deposit more uniformly because single particles (rather than flocs) will undergo deposition; a flocculated layer of particles will not deposit as selectively as single particles. The particles were added dropwise from the pipet to avoid disturbances to the interface and increase the likelihood of particles pinning to the interface. Despite this precaution, a fraction of particles were observed to escape into the water subphase. Thus, the particle coverage cited herein is an upper bound. The particles were allowed to equilibrate for 15 min prior to the start of the deposition. Following equilibration, the ∼2 cm long chip was removed at a velocity of 1 cm/min. Thus, the total deposition process took 2 min. Once fully removed from the fluid, the chip was allowed to dry for a minimum of 10 min prior to removal from the dipper, unless otherwise stated. The chip was placed in a covered petri dish before further processing. All optical microscopy images were captured with a Nikon regular microscope operating in reflection mode, and all scanning electron microscopy (SEM) images were captured with a Philips Scanning Electron Microscope XL30 FEG. Finally, although not the focus of this article, gold nanorods dispersed in water were used to visualize the dynamics of a receding contact line (see Figure 2). The nanorods were obtained from the Colloidal Chemistry Group at Universidade de Vigo, Spain. A sessile drop of a suspension of nanorods suspended with cetyltrimethylammonium bromide (CTAB) was allowed to evaporate from a patterned substrate. Images were captured with a Nikon regular microscope operating in reflection mode.

RESULTS AND DISCUSSION

A. Deposition of Particles onto a Chemically Patterned Substrate. Particles were deposited from a decane−water interface onto a chip with 38 geometries. Each geometry consisted of an array of either circular or square hydrophilic patches, with a characteristic length scale a and separation distance $2s$. The ranges of a and s were from 150−2 μm and 100−2.5 μm, respectively. Figure 4 shows a series of SEM images of three geometries following deposition from an interface with an initial surface coverage of 106%. As noted earlier in the text, the reported surface coverage is an upper bound because a fraction of particles will be lost to the water subphase. The images show square patches with a = 5 μm and s = 3 μm, squares patches with a = 50 μm and s = 15 μm, and circle patches with a = 15 μm and s = 50 μm.

Figure 4A,B demonstrates the uniformity and selectivity of the deposition process. Particles were deposited on every hydrophilic patch in view, with no particles depositing onto the hydrophobic regions. For example, there are no empty patches of the ∼1300 shown in Figure 4B. Similarly, particles selectively deposited onto the larger hydrophilic patches shown in Figure 4C,D. The number of particles deposited onto each patch was proportional to patch size at these conditions. Small clusters of particles (< 10 particles) with no apparent shape preference were formed on the small patches (a = 5 μm), while larger aggregated groups of particles (∼800 particles) formed on the large patches (a = 50 μm). Deposition of particles occurred only on patches because of the difference in wetting between the hydrophilic and hydrophobic regions. During LB deposition, the three-phase contact line will intersect the substrate with an equilibrium contact angle θ_c that satisfies the boundary conditions set by the fluids and substrate. When θ_c approaches 0°, a thin film of fluid will be entrained along the substrate in the hydrophilic regions, thereby providing an avenue for particle deposition.

Upon deposition, particles did not maintain the ordered structure found at the decane−water interface. Rather, particles were attracted to their neighbors and aggregated upon deposition because of immersion capillary attraction.[44−47] Once proximate to the substrate, particles were unable to relieve local curvature in the interstitial fluid via longitudinal movement. Thus, undulations in contact line, or other effects that may cause curvature in the interstitial fluid, caused particles to attract each other to minimize interfacial distortion (see Figure 5).[47] The energy of attraction associated with this clustering process for micrometer scale particles is on the order of ∼10^6 kT.[44] Clustering could be avoided by lowering the energy of attraction through altering the wetting properties of the particles either through addition of surfactant or a cosolvent.

B. Tuning the Size of Clusters with Template Geometry. The experiments described above produced a mixture of colloidal clusters of varying size (from 4−1000 particles) in a single experiment. It is often more desirable to synthesize clusters of approximately the same size, thereby utilizing the entire chip and also avoiding the need for downstream size separation of clusters. We achieved this by fabricating a wafer containing chips that each had one geometry (rather than 38). The LB deposition experiments were conducted in the same way on a chip of square patches with a = 7.5 μm and s = 2.5 μm. Figure 6 shows two micrographs of a chip following deposition from a decane−water interface with

DOI: 10.1021/la504383m
Langmuir 2015, 31, 1632−1640

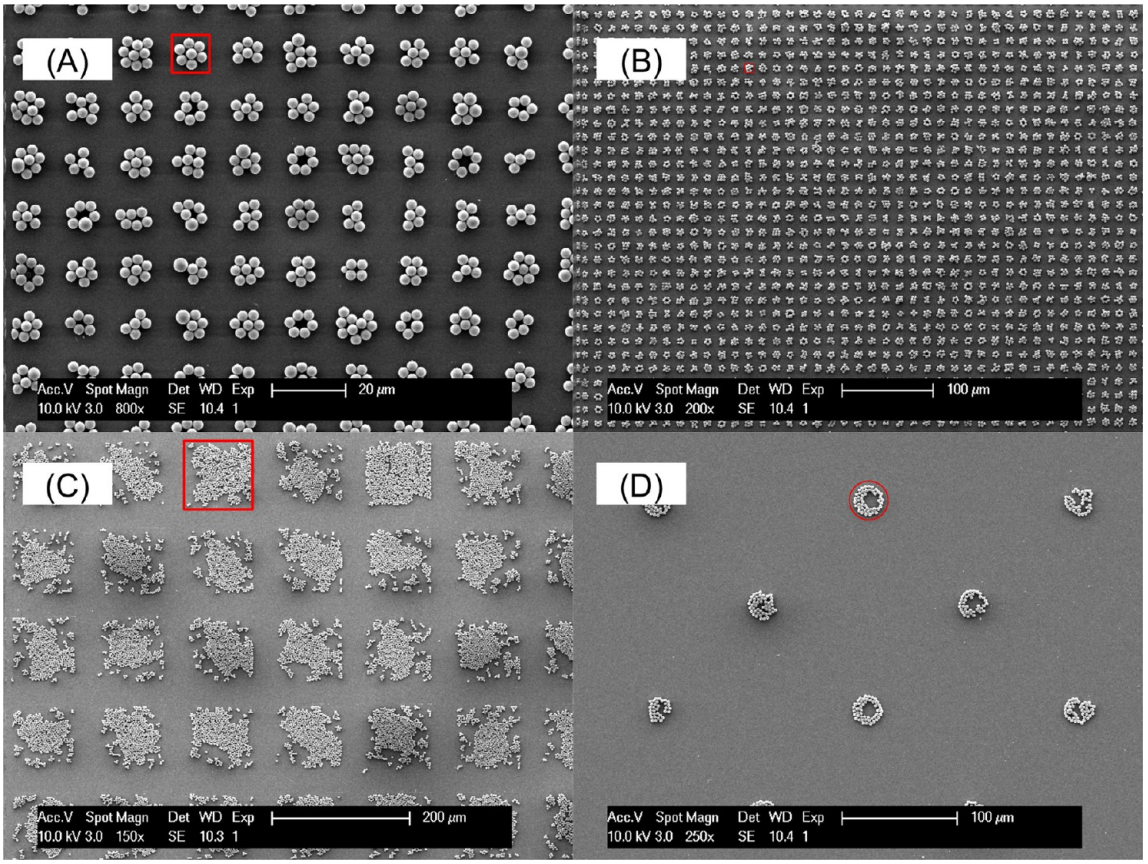

Figure 4. SEM images of particles deposited onto chips of varying geometry. The red outline indicates the boundary of the hydrophilic patch in all panels. (A,B) Square hydrophilic patches with a = 5 μm and s = 3 μm. These images show a highly selective deposition, when colloidal particles were uniformly deposited onto the hydrophilic patches across the whole geometry. (C) Square hydrophilic patches with a = 50 μm and s = 15 μm and (D) circular hydrophilic patches with a = 15 μm and s = 50 μm.

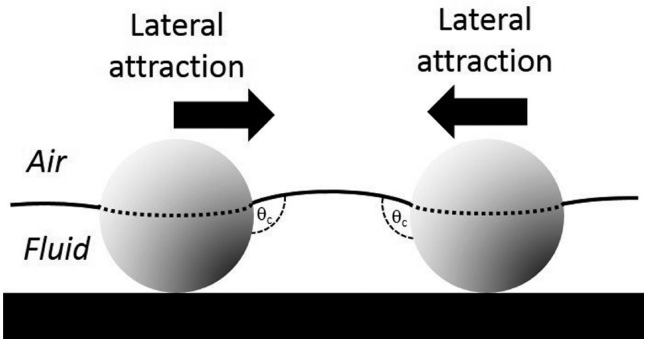

Figure 5. Particle aggregation during drying from immersion capillary attraction. Particles aggregated with their neighbors because of immersion capillary attraction caused by local deformations in the interface. The interface between the interstitial fluid and air is deformed because of the wetting conditions on the surface of the particle dictated by the particle contact angle θ_c.

an initial particle surface coverage of 70%. As in the experiments previously described, particle deposition was quite uniform. Figure 6C shows a histogram of particle cluster size from this deposition and also a deposition from the multigeometry chip, with geometries of a = 7.5 μm and s = 2.5 μm and a = 5 μm and s = 3 μm, respectively. The number-average cluster size or "molecular weight" M_n for clusters synthesized with the two geometries were 12.74 and 6.25 particles/clusters for the first and second geometry, respectively. Further, both depositions produced clusters that had low size dispersity (SD, formerly PDI)[48] = 1.01 and 1.03 for the large and small clusters, respectively. The uniformity in the number of particles deposited onto each patch would likely increase if the procedure was conducted at constant surface pressure, as is often done with LB deposition. However, it is unknown if uniformity in the configuration of particle clusters would also increase.

The direct effect of patch size on cluster size was clear, but the effect of the reduced spring constant k/κ (see eq 3) was subtler. Recall that the reduced spring constant depends only on the characteristic length scale and separation distance of the patches comprising the pattern. The impact of k/κ on cluster size was tested for patches of uniform characteristic size, but different geometry. The number of particles deposited onto circular and square patches with a = 15 μm as a function of geometry was tallied for three different initial surface coverages and varying k/κ. Figure 1 in the SI shows the number of particles on each patch plotted as a function of k/κ.

The data in SI Figure 1 is highly variable, but shows a trend that the number of particles deposited onto a single patch roughly scaled with reduced spring constant when $k/\kappa > 1$. One possible reason for this dependence was in the movement of particles away from a hydrophilic patch when the contact line was locally deformed. At small reduced spring constant, the contact line was able to sustain a larger local deformation than when the reduced spring constant was large. Particles are more likely to move toward the minimum in the contact line

DOI: 10.1021/la504383m
Langmuir 2015, 31, 1632−1640

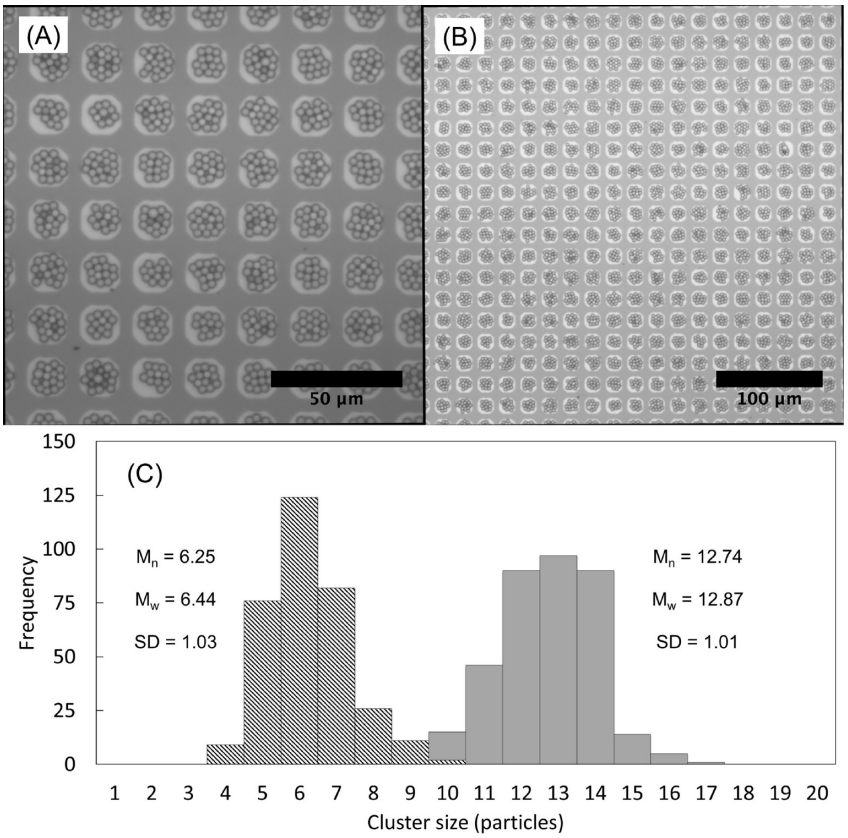

Figure 6. Deposition onto chip of single geometry. (A,B) Colloidal particles were deposited onto a chip with a = 7.5 μm and s = 2.5 μm over an array with total area of 60 mm^2 or 150 000 patches. (C) Particle distributions for patches with a = 5 μm and s = 3 μm (crossed pattern, see Figure 4B) and a = 7.5 μm and s = 2.5 μm (solid gray, panel B); the number-average "molecular weight" M_n for particles synthesized with the two geometries were 6.25 and 12.74 particles/cluster for the first and second geometry, respectively. Both geometries produced clusters that had low size dispersity (SD) = 1.03 and 1.01.

deformation at these conditions, thereby lowering the concentration of particles available to deposit at small k/κ. This hypothesis, however, is not supported by experimental data when $k/\kappa < 1$, where the trend of particle deposition scaling with reduced spring constant was reversed for two of the five cases. One possible explanation for this behavior is that there is deviation from the linear approximation shown in eqs 2 and 3 at large deformation. Further complicating this analysis was heterogeneity in the size of particles. The number of particles a single patch can accommodate will clearly depend on the size of individual particles. Thus, the size dispersity in an ensemble of colloidal particles contributes to dispersity in the number of particles deposited onto a patch. Further, previous work has shown the heterogeneous nature of the repulsive interaction between particles pinned at a water−oil interface,[40] which may also contribute to the variability of results found in SI Figure 1. Clearly, additional experiments need to be conducted to substantiate the subtle effect of k/κ. A larger variety of shapes of increasing complexity should be tested to determine whether the effect is generally applicable or specific to the simple shapes tested herein. Establishing the relationship between the number of deposited particles and k/κ provide guidance for the design of patches.

C. Annealing and Redispersal of Planar Colloidal Clusters. Neighboring particles were permanently bonded via partial coalescence following deposition by heating the chips above the polystyrene glass transition of ∼100 °C. SEM images of a particle doublet, triplet, quadruplet, and quintuplet are shown in Figure 7. Particles that were annealed for longer times coalesced to a larger extent, thereby distorting away from spheres (see Figure 2 in the SI). Previous work from other groups has shown that the portion of the particle in contact with the substrate may flatten during the annealing process,[49] but we did not image the bottom of clusters to determine the presence (or absence) of a flat bottom. Next, the substrate (with annealed clusters) was placed in a 1.5 mL centrifuge tube of ultrapure water. The centrifuge tube was then placed in a bath sonicator for 2 h to separate the annealed clusters from the substrate. Typically, the majority of clusters were removed after 2 h, but the process was repeated until all clusters were removed. The dilute suspension of colloidal clusters was centrifuged and were readily redispersed in either a small volume (<2 mL) of ultrapure water or a mixture of 70:30 ultrapure water:IPA.

Figure 8 shows bonded colloidal clusters dispersed in the bulk (Figure 8A−C) and at a decane−water interface containing isotropic particles (Figure 8D−F). Clusters were stable against flocculation in both systems, indicating that there was likely no significant change in the surface chemistry of the particles as a result of the processing. Although great care was taken in the addition of colloidal clusters to the fluid−fluid interface, the majority of large clusters were lost to the water subphase. Still, a small fraction of clusters remained at the decane−water interface for examination. Figure 8D−F show that strong dipolar repulsion remained between clusters and isotropic particles. The strong dipolar force dominated the

DOI: 10.1021/la504383m
Langmuir 2015, 31, 1632−1640

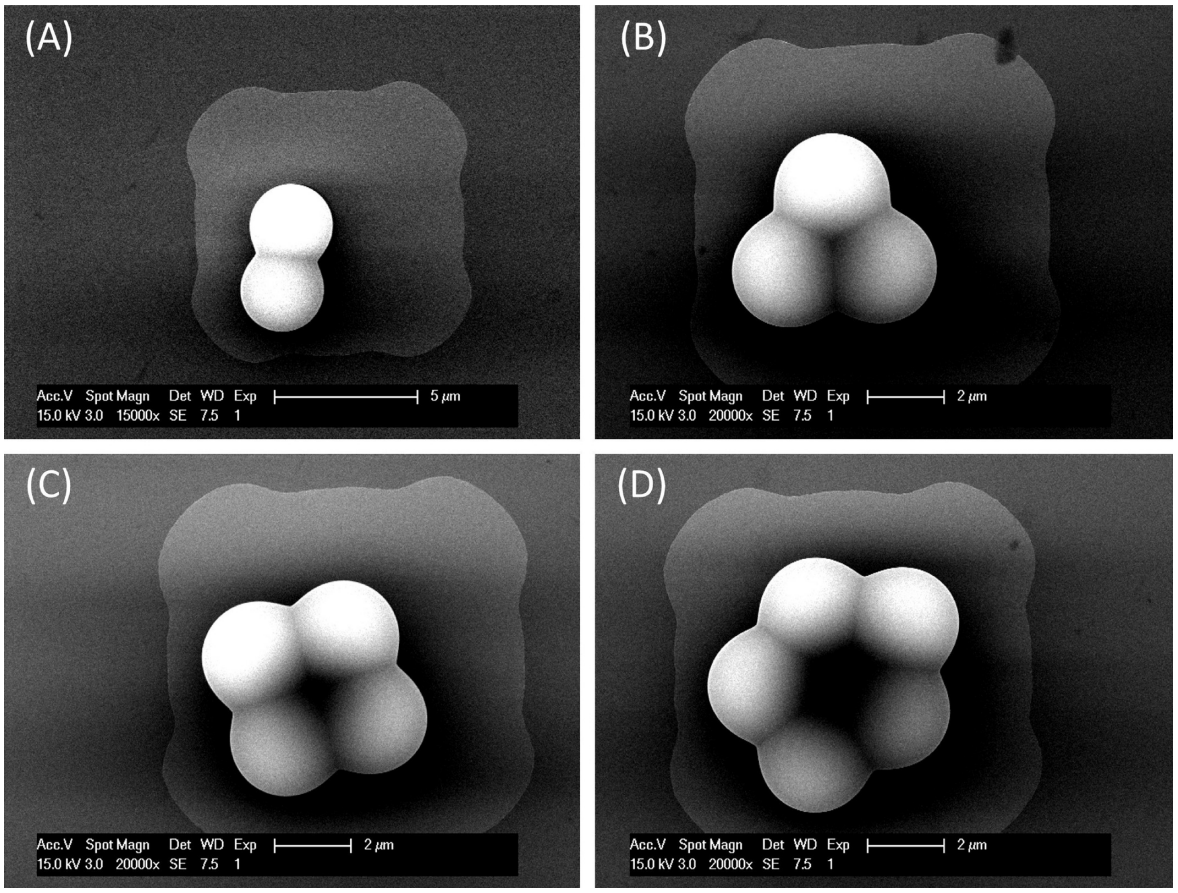

Figure 7. SEM images after annealing of a particle (A) doublet, (B) triplet, (C) quadruplet, and (D) quintuplet. The particles were distorted away from spheres following annealing.

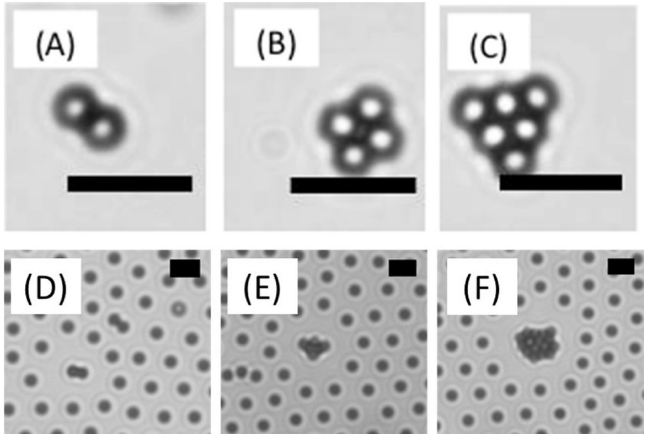

Figure 8. Planar colloidal clusters dispersed in the bulk (A–C) and at a decane–water interface (D–F). The clusters were stable in water and at a decane–water interface. Surprisingly, the dipolar repulsion was much stronger than the capillary attraction between anisotropic clusters and isotropic particles pinned at the decane–water interface (D–F).

capillary attraction that small (low Bond number) anisotropic particles (such as ellipsoids) typically experience with neighboring particles because of local deformations in contact line caused by the need to satisfy the particle's wetting boundary condition.[50] One possible explanation is that there is little to no local deformation in the contact line as a consequence of the clusters' anisotropic shape because the particle contact angle is equal to or close to 90°; the decane–water contact angle for these particles was previously reported 90° ± 20°.[41] Nevertheless, the continued presence of strong repulsion between isotropic colloids and clusters illustrates that the surface chemistry of the particles has not been altered significantly during processing. Given that they were readily dispersed at the decane–water interface, the colloidal clusters could be a useful model system to study the orientation of nonspherical particles at a fluid–fluid interface.[51−53]

■ CONCLUSIONS

The synthesis of colloidal clusters is relevant both as a model system for molecular interactions as well as the fabrication of advanced materials. We described a technique for the simple and fast synthesis of planar colloidal clusters. By combining two existing strategies for colloidal assembly, chemical modification of a substrate and LB deposition from a fluid–fluid interface, we were able to assemble isotropic colloidal particles into clusters of uniform, but arbitrary size. In addition, we found that the number of particles deposited onto each patch depended on the geometry of the hydrophilic pattern. The advantages of the process is that it requires very simple lithography procedures, can make colloidal clusters of various sizes in a single cycle, and is applicable to a wide range of particles. The only requirements are that particles are stable at an interface and can be permanently bonded following deposition by annealing above a glass transition temperature. Thus, this process could be used to produce a variety of model anisotropic systems comprising isotropic particles with, for

DOI: 10.1021/la504383m
Langmuir 2015, 31, 1632–1640

example, florescent or magnetic domains. Although low size dispersity colloidal clusters were fabricated, the primary disadvantage of this process is the current lack of control over the structure of the colloidal cluster. In future work, increasing the geometric complexity of the hydrophilic patch may help to guide structures of the clusters and guide their self-assembly into complex forms.

■ ASSOCIATED CONTENT

Supporting Information

Section A of the SI contains data from experiments testing the effect of reduced spring constant on cluster size. Section B of the SI contains microscopy images of colloidal clusters following annealing. Section C of the SI is a section describing the regeneration procedure for the chip template. This material is available free of charge via the Internet at http://pubs.acs.org.

■ AUTHOR INFORMATION

Corresponding Author

*E-mail: c.wirth@csuohio.edu.

Present Address

[‖]Chemical and Biomedical Engineering Department, Washkewicz College of Engineering, Cleveland State University, 2121 Euclid Ave., Cleveland, OH 44115.

Author Contributions

The manuscript was written through contributions of all authors. All authors have given approval to the final version of the manuscript.

Notes

The authors declare no competing financial interest.

■ ACKNOWLEDGMENTS

The authors thank Professor Luis M. Liz-Marzan, head of the Colloidal Chemistry Group at Universidade de Vigo, Spain, for the gold nanorod suspension. The research was performed as part of the IAP program MICROMAST financed by BELSPO. The FWO Vlaanderen, projects G.0554.10 and G.0697.11, as well as the ERC starting grant 337739 - HIENA are gratefully acknowledged for their financial support.

■ REFERENCES

(1) Manoharan, V. N.; Elsesser, M. T.; Pine, D. J. Dense packing and symmetry in small clusters of microspheres. *Science* **2003**, *301*, 483.

(2) Xia, Y.; Yin, Y.; Lu, Y.; McLellan, J. Template-assisted self-assembly of spherical colloids into complex and controllable structures. *Adv. Funct. Mater.* **2003**, *13*, 907−918.

(3) Zhang, J.; Li, Y.; Zhang, X.; Yang, B. Colloidal self-assembly meets nanofabrication: From two-dimensional colloidal crystals to nanostructure arrays. *Adv. Mater.* **2010**, *22*, 4249−69.

(4) Duguet, E.; Désert, A.; Perro, A.; Ravaine, S. Design and elaboration of colloidal molecules: An overview. *Chem. Soc. Rev.* **2011**, *40*, 941−60.

(5) Li, F.; Josephson, D. P.; Stein, A. Colloidal assembly: The road from particles to colloidal molecules and crystals. *Angew. Chem., Int. Ed. Engl.* **2011**, *50*, 360−88.

(6) Yin, Y.; Lu, Y.; Gates, B.; Xia, Y. Template-assisted self-assembly: A practical route to complex aggregates of monodispersed colloids with well-defined sizes, shapes, and structures. *J. Am. Chem. Soc.* **2001**, *123*, 8718−29.

(7) Blaaderen, A. Van Chemistry. Colloidal molecules and beyond. *Science* **2003**, *301*, 470−1.

(8) Zerrouki, D.; Baudry, J.; Pine, D.; Chaikin, P.; Bibette, J. Chiral colloidal clusters. *Nature* **2008**, *455*, 380−2.

(9) Zerrouki, D.; Rotenberg, B.; Abramson, S.; Baudry, J.; Goubault, C.; Leal-Calderon, F.; Pine, D. J.; Bibette, J. Preparation of doublet, triangular, and tetrahedral colloidal clusters by controlled emulsification. *Langmuir* **2006**, *22*, 57−62.

(10) Kim, J.; Larsen, R. J.; Weitz, D. A. Synthesis of nonspherical colloidal particles with anisotropic properties. *J. Am. Chem. Soc.* **2006**, *128*, 14374−7.

(11) Zhang, Z.; Pfleiderer, P.; Schofield, A. B.; Clasen, C.; Vermant, J. Synthesis and directed self-assembly of patterned anisometric polymeric particles. *J. Am. Chem. Soc.* **2011**, *133*, 392−5.

(12) Grzelczak, M.; Vermant, J.; Furst, E. M.; Liz-Marzán, L. M. Directed self-assembly of nanoparticles. *ACS Nano* **2010**, *4*, 3591−605.

(13) Sacanna, S.; Irvine, W. T. M.; Chaikin, P. M.; Pine, D. J. Lock and key colloids. *Nature* **2010**, *464*, 575−8.

(14) Wang, Y.; Wang, Y.; Breed, D. R.; Manoharan, V. N.; Feng, L.; Hollingsworth, A. D.; Weck, M.; Pine, D. J. Colloids with valence and specific directional bonding. *Nature* **2012**, *491*, 51−5.

(15) Aizenberg, J.; Braun, P.; Wiltzius, P. Patterned Colloidal Deposition Controlled by Electrostatic and Capillary Forces. *Phys. Rev. Lett.* **2000**, *84*, 2997−3000.

(16) Koo, H. Y.; Yi, D. K.; Yoo, S. J.; Kim, D.-Y. A Snowman-like Array of Colloidal Dimers for Antireflecting Surfaces. *Adv. Mater.* **2004**, *16*, 274−277.

(17) Zheng, H.; Rubner, M. F.; Hammond, P. T. Particle Assembly on Patterned "Plus/Minus" Polyelectrolyte Surfaces via Polymer-on-Polymer Stamping. *Langmuir* **2002**, *18*, 4505−4510.

(18) Jonas, U.; del Campo, A.; Krüger, C.; Glasser, G.; Boos, D. Colloidal assemblies on patterned silane layers. *Proc. Natl. Acad. Sci. U. S. A.* **2002**, *99*, 5034−9.

(19) Rycenga, M.; McLellan, J. M.; Xia, Y. Controlling the Assembly of Silver Nanocubes through Selective Functionalization of Their Faces. *Adv. Mater.* **2008**, *20*, 2416−2420.

(20) Zheng, H.; Berg, M. C.; Rubner, M. F.; Hammond, P. T. Controlling cell attachment selectively onto biological polymer-colloid templates using polymer-on-polymer stamping. *Langmuir* **2004**, *20*, 7215−22.

(21) Kuemin, C.; Nowack, L.; Bozano, L.; Spencer, N. D.; Wolf, H. Oriented assembly of gold nanorods on the single-particle level. *Adv. Funct. Mater.* **2012**, *22*, 702−708.

(22) Thai, T.; Zheng, Y.; Ng, S. H.; Mudie, S.; Altissimo, M.; Bach, U. Self-assembly of vertically aligned gold nanorod arrays on patterned substrates. *Angew. Chem., Int. Ed. Engl.* **2012**, *51*, 8732−5.

(23) Duggal, R.; Hussain, F.; Pasquali, M. Self-assembly of single-walled carbon nanotubes into a sheet by drop drying. *Adv. Mater.* **2006**, *18*, 29−34.

(24) Li, Q.; Zhu, Y. T.; Kinloch, I. A.; Windle, A. H. Self-organization of carbon nanotubes in evaporating droplets. *J. Phys. Chem. B* **2006**, *110*, 13926−30.

(25) Giner-Casares, J. J.; Liz-Marzán, L. M. Plasmonic nanoparticles in 2D for biological applications: Toward active multipurpose platforms. *Nano Today* **2014**, *9*, 365−377.

(26) Bao, R.-R.; Zhang, C.-Y.; Zhang, X.-J.; Ou, X.-M.; Lee, C.-S.; Jie, J.-S.; Zhang, X.-H. Self-assembly and hierarchical patterning of aligned organic nanowire arrays by solvent evaporation on substrates with patterned wettability. *ACS Appl. Mater. Interfaces* **2013**, *5*, 5757−62.

(27) Ray, M. A.; Shewmon, N.; Bhawalkar, S.; Jia, L.; Yang, Y.; Daniels, E. S. Submicrometer surface patterning using interfacial colloidal particle self-assembly. *Langmuir* **2009**, *25*, 7265−70.

(28) Bhawalkar, S. P.; Qian, J.; Heiber, M. C.; Jia, L. Development of a colloidal lithography method for patterning nonplanar surfaces. *Langmuir* **2010**, *26*, 16662−6.

(29) Bardosova, M.; Pemble, M. E.; Povey, I. M.; Tredgold, R. H. The Langmuir−Blodgett approach to making colloidal photonic crystals from silica spheres. *Adv. Mater.* **2010**, *22*, 3104−24.

(30) Duffela, B. Van; Ras, R. H. A.; Schryver, C. De; Schoonheydt, R. A. Langmuir−Blodgett deposition and optical diffraction of two-dimensional opal. *J. Mater. Chem.* **2001**, *11*, 3333−3336.

DOI: 10.1021/la504383m
Langmuir 2015, 31, 1632−1640

(31) Tolnai, G.; Csempesz, F.; Kabai-Faix, M.; Kálmán, E.; Keresztes, Z.; Kovács, A. L.; Ramsden, J. J.; Hórvölgyi, Z. Preparation and characterization of surface-modified silica-nanoparticles. *Langmuir* **2001**, *17*, 2683−2687.
(32) Muramatsu, K.; Takahashi, M.; Tajima, K.; Kobayashi, K. Two-dimensional assemblies of colloidal SiO_2 and TiO_2 particles prepared by the Langmuir−Blodgett technique. *J. Colloid Interface Sci.* **2001**, *242*, 127−132.
(33) Isa, L.; Kumar, K.; Müller, M.; Grolig, J.; Textor, M.; Reimhult, E. Particle lithography from colloidal self-assembly at liquid−liquid interfaces. *ACS Nano* **2010**, *4*, 5665−70.
(34) Sastry, M.; Rao, M.; Ganesh, K. N. Electrostatic assembly of nanoparticles and biomacromolecules. *Acc. Chem. Res.* **2002**, *35*, 847−855.
(35) Fan, F.; Stebe, K. J. Assembly of colloidal particles by evaporation on surfaces with patterned hydrophobicity. *Langmuir* **2004**, *20*, 3062−7.
(36) Fan, F.; Stebe, K. J. Size-selective deposition and sorting of lyophilic colloidal particles on surfaces of patterned wettability. *Langmuir* **2005**, *21*, 1149−52.
(37) Dubov, A. L.; Teisseire, J.; Barthel, E. Elastic instability and contact angles on hydrophobic surfaces with periodic textures. *Europhys. Lett.* **2012**, *97*, 26003.
(38) Joanny, J. F.; de Gennes, P. G. A model for contact angle hysteresis. *J. Chem. Phys.* **1984**, *81*, 552.
(39) Gauthier, A.; Rivetti, M.; Teisseire, J.; Barthel, E. Role of kinks in the dynamics of contact lines receding on superhydrophobic surfaces. *Phys. Rev. Lett.* **2013**, *110*, 046101.
(40) Park, B. J.; Vermant, J.; Furst, E. M. Heterogeneity of the electrostatic repulsion between colloids at the oil−water interface. *Soft Matter* **2010**, *6*, 5327.
(41) Masschaele, K.; Park, B. J.; Furst, E. M.; Fransaer, J.; Vermant, J. Finite ion-size effects dominate the interaction between charged colloidal particles at an oil−water interface. *Phys. Rev. Lett.* **2010**, *105*, 048303.
(42) Park, B. J.; Pantina, J. P.; Furst, E. M.; Oettel, M.; Reynaert, S.; Vermant, J. Direct measurements of the effects of salt and surfactant on interaction forces between colloidal particles at water−oil interfaces. *Langmuir* **2008**, *24*, 1686−94.
(43) Wirth, C. L.; Furst, E. M.; Vermant, J. Weak electrolyte dependence in the repulsion of colloids at an oil−water interface. *Langmuir* **2014**, *30*, 2670−5.
(44) Kralchevsky, P. A.; Nagayama, K. Capillary interactions between particles bound to interfaces, liquid films, and biomembranes. *Adv. Colloid Interface Sci.* **2000**, *85*, 145−192.
(45) Denkov, N.; Velev, O.; Kralchevsky, P.; Ivanov, I.; Yoshimura, H.; Nagayama, K. Mechanism of formation of two-dimensional crystals from latex particles on substrates. *Langmuir* **1992**, *8*, 3183−3190.
(46) Lazarov, G. S.; Denkov, N. D.; Velev, O. D.; Kralchevsky, P. A.; Nagayama, K. Formation of two-dimensional structures from colloidal particles on fluorinated oil substrate. *J. Chem. Soc., Faraday Trans.* **1994**, *90*, 2077.
(47) Kralchevsky, P. A.; Denkov, N. D. Capillary forces and structuring in layers of colloid particles. *Curr. Opin. Colloid Interface Sci.* **2001**, *6*, 383−401.
(48) Stepto, R. F. T. Dispersity in polymer science (IUPAC Recommendations 2009). *Pure Appl. Chem.* **2009**, *81*, 351−353.
(49) Ramírez, L. M.; Milner, S. T.; Snyder, C. E.; Colby, R. H.; Velegol, D. Controlled flats on spherical polymer colloids. *Langmuir* **2010**, *26*, 7644−9.
(50) Loudet, J.; Alsayed, A.; Zhang, J.; Yodh, A. Capillary interactions between anisotropic colloidal particles. *Phys. Rev. Lett.* **2005**, *94*, 018301.
(51) Park, B. J.; Choi, C.-H.; Kang, S.-M.; Tettey, K. E.; Lee, C.-S.; Lee, D. Geometrically and chemically anisotropic particles at an oil−water interface. *Soft Matter* **2013**, *9*, 3383.
(52) Park, B. J.; Lee, D. Equilibrium orientation of nonspherical Janus particles at fluid−fluid interfaces. *ACS Nano* **2012**, *6*, 782−90.
(53) Park, B. J.; Lee, D. Configuration of nonspherical amphiphilic particles at a fluid−fluid interface. *Soft Matter* **2012**, *8*, 7690.

DOI: 10.1021/la504383m
Langmuir 2015, 31, 1632−1640